MODELING OF UNSTEADY AERODYNAMIC CHARACTERISTCS OF DELTA WINGS.

Jouannet Christopher, Krus Petter
Linköpings University

Keywords: *Delta wings, Unsteady, Modeling, Preliminary design, Aerodynamic coefficient.*

Abstract

An analytic prediction model is presented to estimate aerodynamic coefficient of delta wing undergoing dynamic motions. The model is based on the introduction of a state space variable describing the vortex breakdown. This model will be suitable for modeling of flight dynamics in the preliminary design phase.

1 Introduction

High angles of attack region becomes more accessible to modern aircraft. Therefore, mathematical modeling of the unsteady aerodynamic forces and moments play an important role in aircraft dynamic investigation and stability analysis at high angles of attack.

The model concentrate on the determination of lift, normal force, drag and moment coefficient for slender delta wings. The present method is compare with published data to ensure agreement between mathematics and test cases.

The present method is based on Polhamus leading edge suction analogy, with integration of the work realized by Traub [3]

Conventional mathematical model based on aerodynamic derivative concept is widely used in flight dynamic, but limitations of this method have been shown by Greenwell [1]. This approach is therefore based on the state-space representation used by Goman [2].

2 Method

The methodology used in this paper is based on the hypothesis that the aerodynamic properties of a delta wing, lift, drag, and pitching moment, basically can be described by three states, that by themselves are rather well understood. These are potential lift, vortex lift and fully separated flow. Therefore, a critical factor in aerodynamic modeling is the transitions between these states that are described by internal state-variables. These transitions describe the stall behavior and much of the unsteady behavior of the wing.

2.1 State-Space variable

The nature of the flow field over slender delta wing, characterized by two vortices that appear at the apex, is suitable for using internal state space variables. The vortex breakdown over the slender delta wing can be defined by a non-dimensional coordinate $x \in [0,1]$. Where x is represented by the following first order differential equation:

$$\tau_1 \cdot \frac{\partial x}{\partial t} + x = x_0(\alpha - \tau_2) \quad \textbf{(1)}$$

τ_1 and τ_2 define the transient aerodynamics effects, τ_1 is the relaxation time constant and τ_2 is the total time delay.

The driving function $x_0(\alpha)$ can be obtain by wind or water tunnel measurements, in the present model the following function is used:

$$x_0(\alpha) = \frac{1}{1 + e^{\sigma \cdot (\alpha - \alpha^*)}} \quad \textbf{(2)}$$

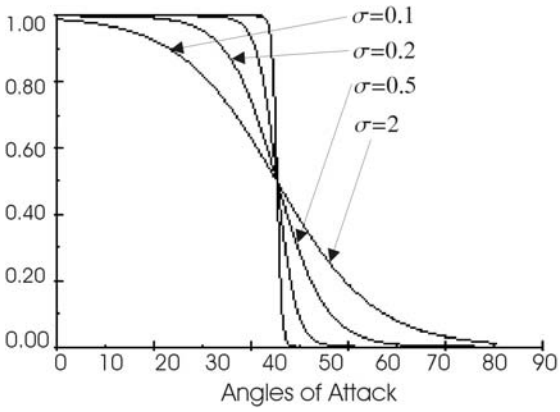

Figure 1 Steady-state separation function for α* =40°

2.2 Lift coefficient

The lift coefficient is based on Polhamus [4] leading-edge suction analogy, with some variation exposed by Jouannet [5]. Polhamus describe the total lift over slender delta wings with two parameters, potential lift and vortex lift, the total lift coefficient is determined by (x)

$$C_L = C_{Lp} + C_{Lv} \quad \textbf{(3)}$$

Where C_{Lp} is the potential lift coefficient defined by:

$$C_{Lp} = k_p \cdot \cos^2 \alpha \cdot \sin \alpha \quad \textbf{(4)}$$

K_p is the potential lift constant, witch can be determined from any lifting surface theory. Traub[3] and Jone[6] presented different evaluation method for K_p. The present model will use:
$K_p = 4 \cdot Tan\varepsilon$ for AR>0,5.

As shown in Jouannet [9] the potential lift is limited to moderated angle of attack, therefore C_{Lp} will be describe by:

$$C_{Lp} = K_p \cdot x_1 \cdot \cos^2 \alpha \cdot \sin \alpha \quad \textbf{(5)}$$

Where x_1 is the attenuation of the potential lift. The other term is the vortex lift obtain by:

$$C_{Lv} = k_v \cdot \cos \alpha \cdot \sin^2 \alpha \quad \textbf{(6)}$$

And K_v is the vortex lift coefficient fixed to π in the present model. The vortex lift is affected by the vortex burst position [7],[8], the internal state space variable for the vortex breakdown is therefore introduced to coupled the vortex lift coefficient to the burst position. The vortex lift is finally expressed by:

$$C_{Lv} = K_v \cdot {x_2}^2 \cdot Sin^2\alpha \cdot Cos\alpha \quad \textbf{(7)}$$

As shown in [5] a third component can be introduced to describe the lift coefficient when the flow is fully separated, no more vortex over the wing. This term is called fully separated lift and is given by:

$$C_{Lfs} = K_{fs} \cdot (1 - x_2) \cdot \cos^2 \alpha \cdot \sin \alpha \quad \textbf{(8)}$$

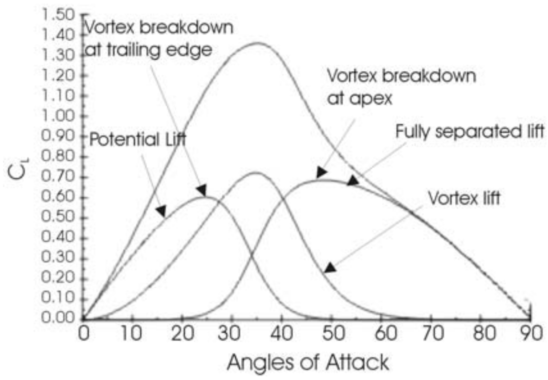

Figure 2 Lift coefficient decomposition

Where x_3 describe the attenuation of the potential flow. And K_{fs} is obtain as half the value of the drag coefficient of a delta wing at 90 degree of angle of attack. K_{fs} can be set a 0.7. K_{fs}=C_{Df}/2
The total lift is describe by:

$$C_L = C_{L0} + C_{Lp} + C_{Lv} + C_{Lfs} \quad \textbf{(9)}$$

The difference between the dynamic and static case is the internal state-space variable. For static case the state-space variable is defined by the following first order differential equation:

$$\tau_1 \cdot \frac{\partial x}{\partial t} + x = x_0(\alpha) \quad \textbf{(10)}$$

During dynamic motions, the differential equation become:

$$\tau_1 \cdot \frac{\partial x}{\partial t} + x = x_0(\alpha - \tau_2 \cdot \alpha') \quad \textbf{(11)}$$

τ_2 and τ_1 can be approximated by $\tau_2 = \frac{c}{2 \cdot V_\infty}$ and $\tau_1 = \frac{15 \cdot c}{V_\infty}$ according to Goman and Khrabov[2].

2.3 Normal force coefficient

The lift coefficient in Polhamus leading edge suction analogy derivate from the normal force, therefore the normal force coefficient can be decomposed in three coefficients in the same way as the lift coefficient. The normal force coefficient is defined by:

$$C_N = C_{Np} + C_{Nv} + C_{Nfs} \quad \textbf{(12)}$$

Where C_{Np} is the potential component, and is expressed by:

$$C_{Np} = K_p \cdot Cos\alpha \cdot Sin\alpha \quad \textbf{(13)}$$

K_p is the same potential coefficient as before. In order to include the normal force decency on the vortex burst position the state-space variable is included in the potential coefficient and gives the following expression:

$$C_{Np} = x_3 \cdot K_p \cdot Cos\alpha \cdot Sin\alpha \quad \textbf{(14)}$$

The second term is related to the normal force due to the vortex. Polhamus defined it as following:

$$C_{Nv} = \frac{C_T}{Cos\Lambda_{LE}} \quad \textbf{(15)}$$

Where C_T is the leading edge thrust coefficient, and it is defined by:

$$C_T = (1 - K_p^2 \cdot K_i) \cdot K_p \cdot Sin^2\alpha \quad \textbf{(16)}$$

K_i is defined by:

$$K_i = \frac{1}{K_p} \cdot \left(1 - \frac{K_v}{K_p \cdot Cos\Lambda_{LE}}\right) \quad \textbf{(17)}$$

K_p and K_v are the same as the one used for lift coefficient. Including K_i in (x) gives the following expression for C_{Nv}:

$$C_{Nv} = \left(1 - K_p + \frac{K_v}{Cos\Lambda_{LE}}\right) \cdot \frac{K_p}{Cos\Lambda_{LE}} \cdot Sin^2\alpha \quad \textbf{(18)}$$

In order to include the dependency of the burst position and the normal force due to the vortex the state-space variable representing the vortex breakdown position is include in the representation of C_{Nv} and gives:

$$C_{Nv} = x_4 \cdot \left(1 - K_p + \frac{K_v}{Cos\Lambda_{LE}}\right) \cdot \frac{K_p}{Cos\Lambda_{LE}} \cdot Sin^2\alpha$$

(19)

The third component is defined as the component due to fully separated flow, when the vortex breakdown has reached the apex, and it is represented by the following equation:

$$C_{Nfs} = C_{Df} \cdot Sin\alpha \quad \textbf{(20)}$$

Where C_{Df} is the drag coefficient of a flat triangular plat perpendicular to the flow. C_{Df} is set to 1.4 in this model. This component of the total normal force coefficient is only active when the burst position reaches the apex, therefore the final expression of C_{Nfs} is given by:

$$C_{Nfs} = (1 - x_5) \cdot C_{Df} \cdot Sin\alpha \quad \textbf{(21)}$$

Where x describe the state of the vortex breakdown.

The final expression for the normal force coefficient is:

$$C_N = C_{Np} + C_{Nv} + C_{Nfs} \quad \textbf{(22)}$$

In the case of dynamic motions the equation is the same, only the first order differential equation representing the vortex breakdown state is changed from:

$\tau_1 \cdot \frac{\partial x}{\partial t} + x = x_0(\alpha)$ to $\tau_1 \cdot \frac{\partial x}{\partial t} + x = x_0(\alpha - \tau_2 \cdot \alpha')$.

The same change as for the lift coefficient.

2.4 Drag Coefficient

The drag coefficient is defined from the lift coefficient and the normal force coefficient.

$$C_D = \frac{C_N - C_L \cdot Cos\alpha}{Sin\alpha} \text{ for } \alpha \neq 0. \quad \textbf{(23)}$$

If α=0 the drag coefficient will be defined by C_{D0}.

2.5 Pitching moment coefficient

The pitching moment is defined from the lift coefficient and the position of the center of pressure.

$$C_m = C_L \cdot \left(x_{cg} - x_{cp}\right) \quad \textbf{(24)}$$

3 Static Cases

This section compare published wind tunnel data with the present models. The main test set is based on the work realized by Wentz [7], often presented as a reference.

3.1 Lift Coefficient

The static results from delta wing with sweep angles from 45 to 55 degree are presented in figure (3).

The present method allows behaviour from low angles of incidence to past stall region to be well captured. At low angles of attack, up to 10 degrees, the present model agreement with the test data is very good. Then up to the stall angle the present prediction over estimates the lift coefficient. For higher angles of attack agreement with experimental data is seen to be very good up to post stall region. In all three cases C_{Lmax} is seen to bee well estimated.

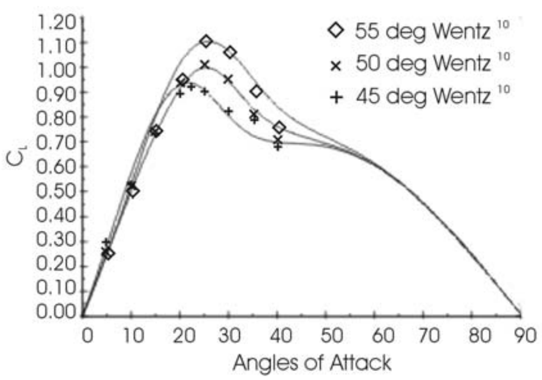

Figure 3 Comparison of theory and present method for 45 to 55 degree delta wing.

For delta wing with sweep angle between 60 and 70 degree, presented in figure (4), the present method shows very good agreement with experimental studies. From low angles of attack up to stall angles the agreement between published data and the present predictions shows very good agreement. At higher angles of incidence, the present model underestimates the published data in the C_{Lmax} region and in early post stall behaviour. But the trend is still in accordance with the test data.

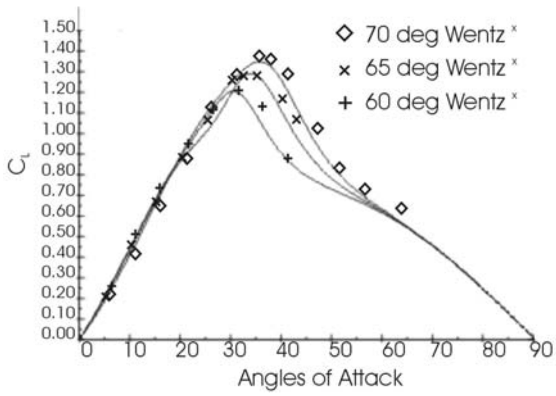

Figure 4 Comparison of theory and present method for 60 to 70 degree delta wing.

The present model match experimental data up to highest angle of attack with available data.

3.2 Normal force Coefficient

The normal force coefficient has only been compare and computed for a 70-degree delta wing. The present model shows very good agreement with test data, figure(5). At low angles of attack the present method over estimates the normal force coefficient.

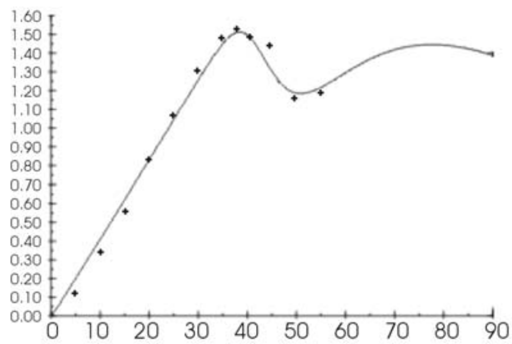

Figure 5 Comparison between test data and present model for the normal force coefficient of a 70-degree delta wing.

At high angles of attack, the present model is underestimating the normal force coefficient, but the trend in post-stall region is in accordance with test data.

3.2 Drag Coefficient

The drag coefficient has been computed for a 70-degree delta wing and compare with published wind tunnel test from Soltani[5].

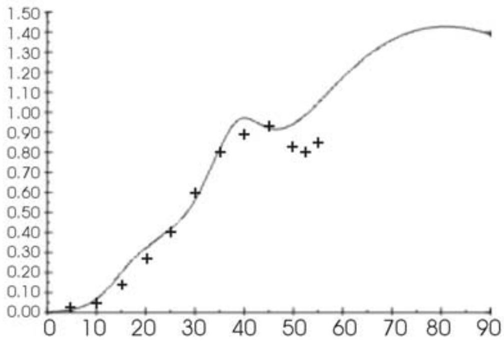

Figure 6 Comparison between test data and present model for a 70-degree delta wing.

Figure (6) illustrates this comparison. The present model shows good agreement with test data. At low angles of attack the present model over estimates the drag coefficient, as for the lift and normal force coefficient. This is a direct result from the modelisation of the drag coefficient.

At high angles of attack, over 25 degree, the present model shows good agreement, but fail to pick up the maximum value at 45 degree. This difference could be seen as the difference observed in the lift coefficient for a 70 degree delta wing in figure(4).

3.3 Pitching Moment Coefficient

The pitching motion in static case has only been computed for a 70-degree delta wing.

At low angles of attack the present model underestimates the pitching moment coefficient, this is mainly due to the modelisation of the location of the center of pressure. At higher angles, over 25 degree the present method present good agreements with the wind tunnel test data.

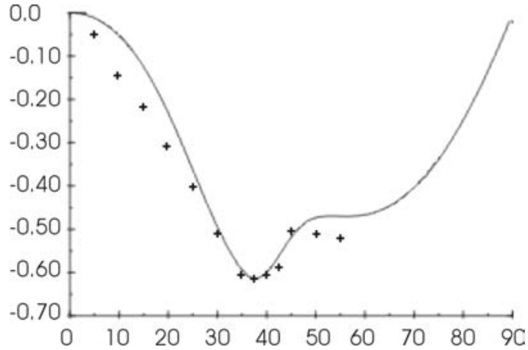

Figure 7 Pitching moment for a 70-degree delta wing.

The accuracy of the model is mainly dependent on the center of pressures model. Improving this one would reduces the differences at low angles of attack.

4 Dynamic Motions

Comparison with test cases has been limited to the study produced by Soltani et al. [9] on 70-degree delta wings.

4.1 Lift Coefficient

Test cases are pitching motions from 0 to 55 degree with different frequencies. Parameters used in the present model are independent from the shifting, and are based on water tunnel results [9].

Figure (8) show comparison between the present model and pitching motions from 0 to 55 degrees of angles of attack with a reduced frequency k=0.072. In figure (8) all the component of the lift coefficient use the same time constant τ_1 and τ_2. During the up stroke motion the present model present a very good agreement with the experimental data, but the maximum value and the stall angle are not well matched. During the down stroke the present model underestimated the lift coefficient.

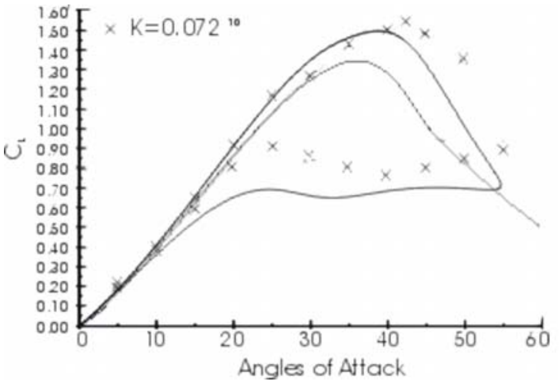

Figure 8 Comparison between experimental data and present method with a reduce frequency k=0.072.

Comparison with other reduced frequency, and variable time constant are presented in [5]. The use of different time constant for the three different state-space variable present very accurate results with the test case, illustrated in figure (9)

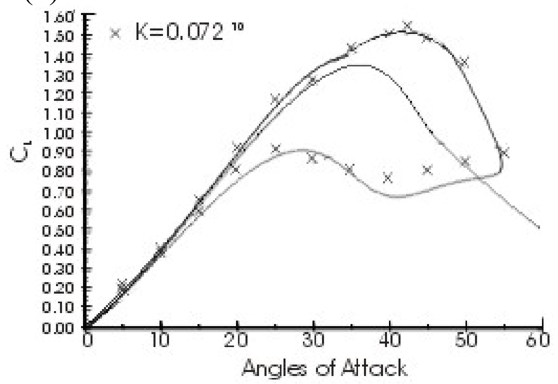

Figure 9 Comparison between test case and the present method with k=0.072. Different time constant for the different input.

The same results have been found for other reduced frequency[5], where the use of different time constant indicates more accurate results.

4.2 Normal Force Coefficient

The normal for determined by the present method have been compare with wind tunnel test present by Soltani[8].

In Figure (10) the normal force coefficient is computed without changing the parameters from the static case, only the pitching rate has been taken into account. The present model over estimates the normal force coefficient during the up stroke, and misses the maximal value. During the down stroke the present model under estimates the coefficient. The trend is respected but there is a deviation from the value.

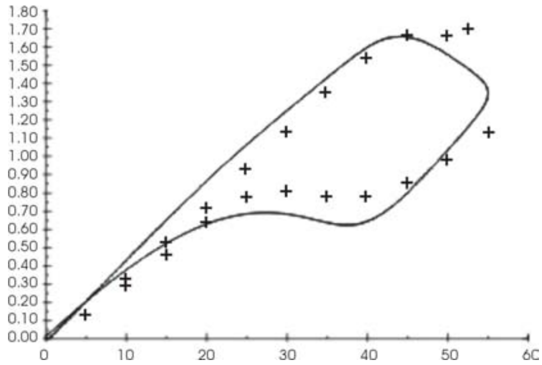

Figure 10 Normal force coefficient for a reduced frequency k=0.072

In figure (11) the normal force is computed for a reduced frequency k=0.165. The same phenomenon as in for the lift coefficient is observed, the present model accuracy increased with increasing reduced frequency.

In figure (11) the present method shows very good agreement with the test data. The maximum value is underestimated, but the trend is respected.

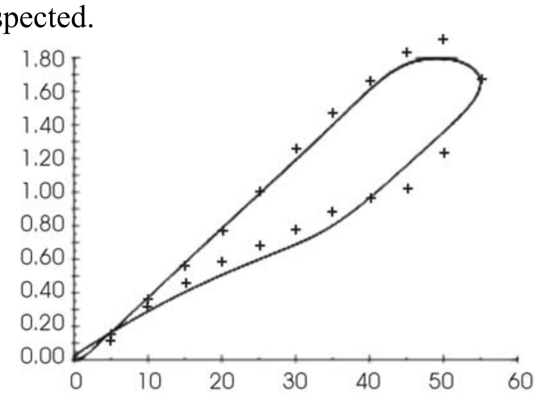

Figure 111 Normal force coefficient for a reduce frequency k=0.165.

As the reduced frequency increased there is less need for different time constant to increase the accuracy of the model.

4.3 Drag Coefficient

Comparison between test data and the present method is presented in figure (13) for a 70-degree delta wing at a reduced frequency k=0.098.

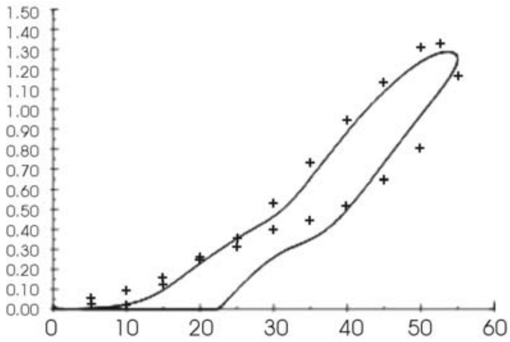

Figure 12 Drag coefficient for a reduce frequency k=0.098,for a 70 degree delta wing.

At low angles of attack the present model indicates poor correlation with the test data. As the angles of attack increase the present model shows better agreement on the up stroke, and acceptable agreement on the first part of the pitch down motion, from maximum angles of attack to 40 degree. Under the correlation is poor.

The drag coefficient is calculated from the lift and the normal force coefficient. As observed for the normal force and the lift coefficient the present model is less accurate at low angles of attack, under 25 degrees, and on the down stroke. This is directly reflected in the drag determination. The drag coefficient accuracy will be improved by improving lift and normal force coefficients.

4.4 Pitching Moment Coefficient

Figure (13) illustrates the comparison between present model and wind tunnel test data from Soltani on a 70 degree delta wing, with a reduced frequency of k=0.072.

At low angles of attack the present model underestimates the pitching moment, as the angle of attack increases the model become more accurate. The present model fails to pick up the maximum. The very simple model for the center of pressure is one of the main explanations for those differences.

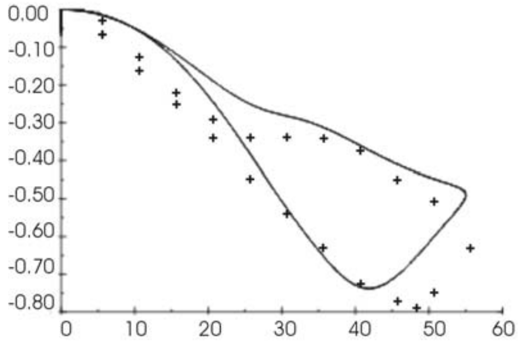

Figure 13 Pitching moment coefficient for a reduced frequency k=0.072.

Figure (13) illustrate the comparison between the present model and wind tunnel test data for a reduce frequency k=0.165.

With higher reduced frequency the accuracy of the present model increase, figure (14). At low angles of attack, up to 25 degree, the present model underestimates the value. This is resulting from the representation of the center of pressures position. At low angles of attack, before the burst reaches the trailing edge, the position of the center of pressure does not agree with reality.

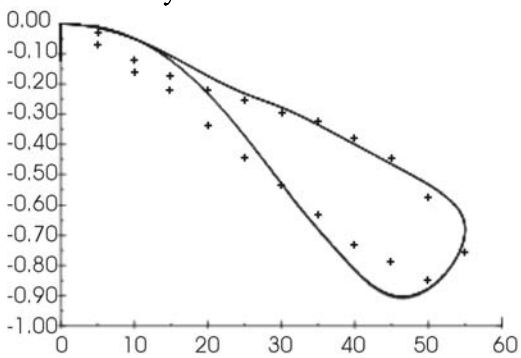

Figure 14 Pitching moment coefficient for a reduced frequency k=0.165.

5 Observation

Prediction of aerodynamic coefficient in static case shows great agreement with published test data, for delta 70-degree delta wing. And could be used for delta wing from 45 degree sweep up to 70 degree sweep, results exposed for the lift coefficient.

During dynamic pitching motions the accuracy of the present method increased with increasing reduced frequency. Present models show good agreement with test data under pitching motion, besides from the drag coefficient, in less magnitude for the pitching motion.

Lift coefficient and normal force coefficient produce very good correlation with published test data in both static and dynamic motion. Showing that the use of steady state variables is a simple and efficient way to produce simple and accurate model for lift, normal force and pitching moment coefficient.

Induced drag has been determined from normal force and lift coefficient. This method shows acceptable value in the static case. During dynamic motion poor agreement is obtain, mostly at low angles of attack and during down stroke motions. This is a direct consequence from the model based on normal force coefficient and lift coefficient. The drag coefficient can be improved by improving both the lift coefficient or the normal force coefficient, or consider other methods to determined it.

Determination of pitching moment has shown good agreement with test data at high alpha in static condition and during dynamic motions. At low angles of attack the present model has poor agreement with test data, this is mostly depending on the modelisation of the center of pressure.

6 Conclusion

A simple model has been presented that predicts the lift, normal force, pitching moment and drag coefficient for a variety of planforms. The present method allows determination of these characteristics, suitable for use in flight dynamic simulation at the preliminary design stage, up to very high angle of attack, including the unsteady behaviour of these characteristics, with an exception for the drag coefficient. It must be noted that the method is based on several simplification and its limitations should be recognized.

Aerodynamic coefficients were determined using the leading edge suction analogy with empirical modification and addition of steady-state variables to describe the vortex breakdown and unsteady behaviour. The method was compare to published experimental results, with very good accuracy being demonstrated in static cases. The unsteady behaviour of aerodynamics coefficients from delta wings have been present and indicated that simple models can describe the trend of the unsteady behaviour and be suitable for conceptual design studies with good confidence. Those models should not been seen as models for use when wind tunnel or flight data are available. The model does, however, contain a sufficient number of degrees of freedom so that the parameters can be adjusted to fit almost any set of data.

7 Summary

The following equation have been determined and used in this paper.

$$C_L = C_{L0} + K_p \cdot x_1 \cdot \cos^2\alpha \cdot \sin\alpha +$$
$$K_v \cdot {x_2}^2 \cdot Sin^2\alpha \cdot Cos\alpha + K_{fs} \cdot (1 - x_2) \cdot \cos^2\alpha \cdot \sin\alpha$$
$$C_N = x_3 \cdot K_p \cdot Cos\alpha \cdot Sin\alpha + (1 - x_5) \cdot C_{Df} \cdot Sin\alpha$$
$$+ x_4 \cdot \left(1 - K_p + \frac{K_v}{Cos\Lambda_{LE}}\right) \cdot \frac{K_p}{Cos\Lambda_{LE}} \cdot Sin^2\alpha$$
$$C_D = x_3 \cdot K_p \cdot Cos\alpha + C_{Df} \cdot (1 - x_5)$$
$$+ x_4 \cdot \left(1 - K_p + \frac{K_v}{Cos\Lambda_{LE}}\right) \cdot \frac{K_p}{Cos\Lambda_{LE}} \cdot Sin\alpha -$$
$$K_p \cdot x_1 \cdot \cos^3\alpha - K_v \cdot {x_2}^2 \cdot Sin\alpha \cdot Cos^2\alpha$$
$$+ K_{fs} \cdot (1 - x_2) \cdot \cos^3\alpha$$
$$\tau_1 \cdot \frac{\partial x}{\partial t} + x = x_0(\alpha)$$
$$x_0(\alpha) = \frac{1}{1 + e^{\sigma \cdot (\alpha - \alpha^*)}}$$

The following coefficient have been used for the 70 degree delta wing:

C_{Df}= 1.4
$\sigma_{1,2,4}$= 0.3
σ_3= 0.5
σ_5= 0.1
α^*_1= 33°
$\alpha^*_{2,3,4}$= 39°
α^*_5= 43°

References

[1] Greenwell, D. I. "Difficulties in the Application of Stability Derivative to the Maneuvering Aerodynamics of Combat Aircraft," ICAS Paper 98-1.7.1, the 21st Congress of the International Council of the Aeronautical Sciences, Sept 1998, Melbourne, Australia.

[2] Goman, M. G. And A. N. Khrabov. "State-Space Representation of Aerodynamic Characteristics of an Aircraft at High Angles of Attack," Journal of Aircraft, Vol. 31, No.5, Sept.-Oct. 1994, pp.1109-1115.

[3] Traub, L. W., "Prediction of Vortex Breakdown and Longitudinal Characteristics of Swept Slender Planforms," Journal of Aircraft, Vol. 34, No 3, May-June 1997.

[4] Polhamus E. C., "A Concept of the Vortex Lift of Sharp-Edge Delta Wings Based on Leading-Edge Suction Analogy," NASA TN D-3767, Oct. 1966

[5] Jouannet, C. and Krus, P. "Lift Coefficient Predictions for Delta Wings Undergoing Pitching Motions", AIAA 2002-2969, 32nd AIAA Fluid Dynamic Conference, June 2002, St Louis, USA.

[6] Jones, R. T., "Properties of Low Aspect Ratio Wings at Speeds Below and Above the Speed of Sound," NACA Rept. 835, 1946, pp59-63

[7] Wentz, W. H., Jr & Kohlman D. L., "Wind Tunnel Investigation of Vortex Breakdown on Slender Sharp-Edged Wings," NASA Research Grant NGR-17-002-043, 1968

[8] Soltani, M. R. & Bragg, M. B. & Brandon, J. M., "Experimental Measurement on an Oscillating 70-degree Delta Wing in Subsonic Flow," AIAA-88-2576-CP, 1998

[9] Jouannet, Ch., "A Water Tunnel Study of Vortical Flows over Delta Wings," Linköpings Universitet, LiTH-IKP-EX-1786, 2001